

## Zhang's Second Order Traffic Flow Model and its Application to The Highway of Kisii – MIGORI



### Engineering

KEYWORDS :

**JAMES MOGIRE  
MBECHE**

Research Scholar, Department of Management, BRA Bihar University, Muzaffarpur,  
Bihar, INDIA

### ABSTRACT

*Macroscopic modeling approach is most suitable for a correct description of traffic flow. In this project we considered the Zhang's second-order macroscopic traffic model and applied it to the Kisii-Migori traffic highway so as to justify it, and study the highway's traffic flow wave phenomenon. The set of partial differential equations governing this Phenomenon were solved using the Finite difference method. The flow problem was solved to show that it is stable, convergent and efficient. The associated Riemann problem was solved to determine the wave propagation in the Traffic flow. Result were analyzed graphically to show the wave propagation in the traffic flow*

### 1.0. INTRODUCTION

Traffic network that consists of highways, streets, and other kind of roadways provide convenient and economical conveyance of passengers and goods. The basic activity in transportation is a trip; defined by its origin, destination, departure time, and arrival time and travel route. Very many trips interact in the network to produce a complicated pattern of traffic flows.

Traffic flow and congestion is a major problem in society and is economically problematic too in both developed and developing countries as far as transportation is concerned. In recent times, much interest has focused on traffic flow models as the amount of traffic on the highways continues to increase. Traffic congestion on motorways is a more pressing problem in countries all over the world, where year in year out, morning and evening during rush hours, the capacity of the roads is exceeded. Traffic jams courses considerable cost due to unproductive time losses beside the possibility of the accidents add the negative effect of environmental air pollution not to mention the health problems, noise and the stressful factors caused by traffic jams. To ease this congestion requires that new and more roads are constructed to Increase the capacity of the infrastructure. However this approach is long term, costly and often faces environmental and societal constraints. Hence the need for short term solution such as traffic control so that congestion is solved, reduced or delayed.

There exists many models nowadays which aim at both safely controlling the traffic and to achieve maximum flow (Hoogendorn and Bovy (2000b)): where the considered models for the vehicle flow can be classified according to the level of details of the flow. Also modeling accuracy, applicability, generality, model calibration and validation has been discussed for each of the categories. Research on the subject of traffic flow modeling was analogized to particles on fluid flow first when Lighthill and Witham (1955) presented a model based on the analogy with vehicle traffic flow with fluid particles. This led to more research and debate for a Mathematical description of traffic flow by traffic engineers, which has resulted to a wider scope of models descriptions as below.

### 1.1. CLASSIFICATION OF TRAFFIC FLOW MODELS

These models were classified according to the level of detail as:

#### 1.1.1. Microscopic

This model describes the space time behavior of the systems entities, vehicles and drivers as well as their interactions individually. For example as for each vehicle in the stream lane-change is described as a detailed chain of drivers decision (Weideman 1974). However this model does not give a summative predictability and is not much of mathematical utility therefore.

#### 1.1.2. Submicroscopic

This model describes the characteristic of individual vehicle in the traffic stream. Also, vehicle control, behavior such as changing gears in correspondence to prevailing surrounding conditions modeled in detail. Further more, the function of specific part (sub-units) of the vehicle is described. Like microscopic model, its shortcoming is lack of dealing with the practical situation on the road's whole traffic flow in a given cell.

Presence, of computers has resulted in development of complex micro-simulation model that distinguish and trace single cars and their drivers. In illustration, the SMARTEST project Algiers *et al* (1997) identified 58 microscopic simulation models of which 55% were analyzed some of which were true microscopic simulations because they model the car-following behavior and the lane changing behavior of each individual vehicle in the traffic flow. Mindehoud (1999) presented a microscopic model SIMONE describing the functioning and the driver operation of an intelligent cruise control (ICC) system, influenced by the direct surrounding of the vehicle. For a review of microscopic and sub microscopic simulation we refer to Alger *et al*

(1997) and minderhoud (1999). Traffic C.M.J, Hoogendoorn, S.P.Van, B (2009) on this theory of continuum reiterated by traffic flow modeling of drivers and support systems in multiclass traffic with intervehicle communication and drivers in the loop. On Kinetic traffic flow model which seems to be a good representation on both the aggregate level-congested dynamics and the level of the individual vehicles-vehicular interaction either directly or thorough intervehicle communication. The human modeling approach is presented.

### 1.1.3. Mesoscopic Flow

This model does not distinguish or trace individual vehicle but do specify the behavior of individuals i.e. in probabilistic terms. Here, traffic is represented by small group of traffic entities, their activities and interactions of which are described at a low detail.

In particular a lane change maneuver might be represented for an individual vehicle as an instantaneous event, where the decision to perform a lane-change is based on for example relative lane densities and speed differentials. Some microscopic models are analogous to gas-kinetic theory. These so-called gas kinetic models describe the dynamics of velocity distributions.

The proponent of this model include Hoogendoorn (1999) who developed a macroscopic, gas kinetic traffic flow model describing the dynamics of generic phase-space density (G-PSD) by presenting dynamic equations that describe how the G-PSD change due to convection, acceleration, smooth adaption of continuous attributes, event-based non-continuum processes (e.g. interaction of traffic entities) and condition based non-continuum processes (e.g. postponed lane changing). The different theories of Prigogine and Herman (1971), pavari-fontana (1975), Helbing(1997),and Hoogendoorn and Bovy (2000a) are all special cases of the genetic model

### 1.1.4. Macroscopic

This model describes traffic at a high level of aggregation as a flow without distinguishing its constituent parts. For example, the traffic stream is represented in an aggregate manner using characteristics as flow rate, density and velocity. Individual; vehicle maneuvers such as a lane change are usually not explicitly represented. A macroscopic model may assume that the traffic stream is properly allocated to the roadway lanes and employ an approximation to this end.

Macroscopic flow models are classified according to the number of partial differential equations that frequently underlies the model on the one hand and there order on the other.

This is because the models are derived from the analogy between vehicular flow and flow of continuous media (fluids or gases); yielding flow models with a limited number of equations that are manageable.

Macroscopic modeling approach is the most suitable for correct description of traffic flow: and increased public attention to this kind of traffic flow modeling is due to the work of Boris Kerner *et al.* (1996), Kerner (1999).

The applicability of this model lies in its capability to replicate how congestion, a phenomenon traffic not desirable but observed in real traffic flow occurring when disturbances are present in transportation systems.

In this research we consider Zhang's second order traffic flow model developed by Zhang (1998) and in Zhang (2000) where a finite difference scheme for this model was developed and then to Kisii Migori town especially in rush hours majorly on Mondays. The Zhang model is a macroscopic traffic flow model; is relatively easier to compute than microscopic models since they only work with aggregate variables. Hence, allowing a fast simulation of the studied motorway that is essential for on line predictive control. Moreover, a macroscopic model is easier to identify and to tune due to the fact that it has fewer parameters to estimate than the microscopic and mesoscopic models.

## 1.2. Literature Review

In the nineteen fifties Lighthill and Whitham (1955), and Richards (1956) separately developed the first dynamics traffic flow model here after referred to as LWR. The LWR model describes the traffic using a conservation law where they assumed that the traffic flow is related to the traffic density. It is a first-order macroscopic traffic flow model since only the density is a variable. Newell (1993) improved the LWR model so as to cope with shockwaves and stop- and- go traffic in congested traffic situations, Payne (1971) proposed the first continuum traffic flow model by a coupled system of two partial differential equations. This system employs the conservation law and the principal of conservation of motion by using a partial differential equation describing the dynamics of velocity. The macroscopic Payne model is of second-order since it has two variables (i) traffic density and (ii) average traffic velocity.

(1996) proposed a third-order macroscopic traffic flow model with the traffic density, the average velocity and the variance on the velocity as variables.

**Remark:** A great deal of work has been devoted to the study of traffic flow by improving on already existing models and / or using various numerical approximation techniques in attempting to give more accurate results Hoogendoorn and Bovy (2006) .

**Verification.** Verification of traffic flow models has also been done Wu and Brilon (1999), Nagel *et al* (1999) and Esser *et al* (1999) verified the microscopic cellular Automaton model on German and American motorways which showed fairly realistic results on a macroscopic scale, especially in the case of urban networks in terms of reproduction of empirical  $v$  speed density curves.

Moreover, Yonnel G. *et al* (2002) used the microscopic model based paramics traffic simulations model to investigate freeway operation on I-680 free way in the San Francisco Bay Area with the aim of obtaining in-depth knowledge of the paramics model for free-way applications developing and evaluating a calibration process, assessing the model's ability to serve as a tool for the evaluating freeway improvement strategies and investigating various improvement strategies for the I-680 study section.

In general, Cremer and Papageorgiou, (1981), Helbing (1997) and Kerner *et al* (2002) shows that macroscopic models are relatively easy to calibrate due to their limited number of parameters and that they feature only some characteristic variables that are largely, independent on roadway geometry, weather etc. Kotsialos *et al* (1999) shows macroscopic traffic flow models are suitable for large simulation of traffic flow in networks where he applied the METANET model to the peri-urban network of the Dutch city of Amsterdam and the Paris network. Corinne (2000), investigated the potentiality of the features of METACOR (a macroscopic Payne-type) traffic flow model for simulating traffic flow on the road network located around the lake Brunnisviken, situated North of Stockholm city, and for designing traffic control strategies for the Swedish traffic conditions. In this study, we considered the Zhang's second-order macroscopic traffic flow developed by Zhang (1998) and Zhang (2000) to Kisii-Migori highway. We also considered Zhang's Godunov finite difference method in solving the model (Zhang 2000a). M.O.Gani *et al* (2011) on a finite difference scheme for a dynamic Traffic flow model appended with two-point boundary condition.

### 1.3. Objectives of the study

1. The wave phenomenon found in traffic flows along many highways was studied using the Zhang's second order traffic flow model.
2. This Zhang's second-order traffic flow model was justified by applying it to the Kisii Migori highway in analyzing the highway's traffic flow situation.

### 1.4. The fundamental diagram

This is an important tool in understanding the relation between the traffic flow and the traffic density at a given location of the motorway. In observing the traffic on a motorway and plotting traffic flow versus traffic density for a location along the motorway a curve such as below emerges. This is the same for every motorway location and is known as 'the fundamental diagram'.

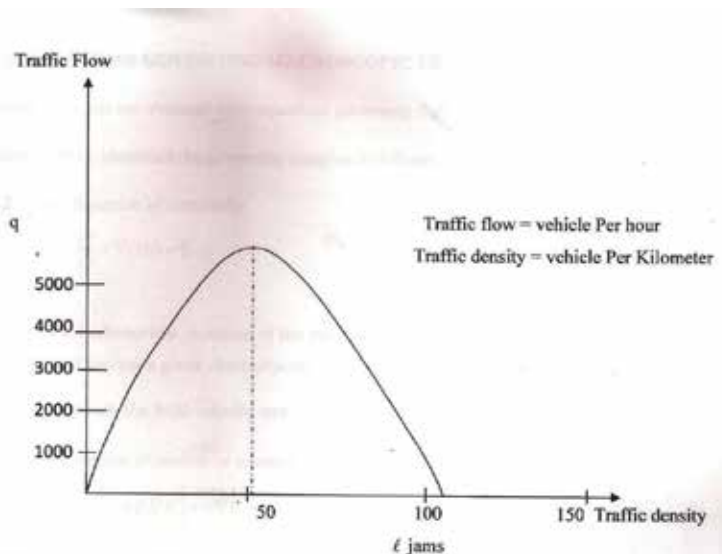


Figure 1

#### 1.4.1 THE FUNDAMENTAL DIAGRAM:

Plotting traffic flow versus traffic density on a motorway resulted in the figure above. The density at which the traffic flow is maximal is density at which the flow equals zero (i.e. the vehicle comes to stand-still) is called jam density ( $\ell$  jam)

## 2.0 EQUATIONS GOVERNING MACROSCOPIC TRAFFIC FLOW

These equations are obtained from equations governing fluid flow in fluid dynamics

Gupta (1991), identified the governing equation as follows:-

2.1. (i) Equation of continuity.

$$\frac{\partial \ell}{\partial t} + \vec{\nabla} \cdot (\ell \vec{v}) = 0 \tag{1}$$

Which is a mathematical equation of the principle of mass conservation.

2.2 (ii) Equation of motion or momentum.

$$\ell \left[ \frac{\partial \vec{v}}{\partial t} + \vec{v} \cdot \vec{\nabla} \vec{v} \right] = -\vec{\nabla} P + \mu \nabla^2 \vec{v} + \ell \vec{F} \tag{2}$$

Which is the Navier-Stokes equation of motion.

Equation (2) represents the principle of conservation of motion that states that the rate of momentum change is equal to the net forces. Given that the highway traffic flows horizontally i.e. in the x-direction only and that the traffic density (number of vehicles per kilometer of the highway)  $\ell$  and traffic velocity (average velocity of the vehicle in the highway)  $v$  depends only on  $x$  and  $t$ , where  $x$  represents the position on the highway and  $t$  is the time, then taking the vehicle in the traffic flow to serve as fluid particles in the fluid flow, we can analyze the flow of traffic using equation (1) and (2) which reduces to

$$\frac{\partial \ell}{\partial t} + \frac{\partial(\ell v)}{\partial x} = 0 \tag{3}$$

Therefore the Zhang's second-order macroscopic traffic flow model is governed by the following equations:-

$$\frac{\partial \ell}{\partial t} + \frac{\partial(\ell v)}{\partial x} = 0 \tag{4}$$

and

$$\frac{\partial \ell}{\partial t} + v \frac{\partial v}{\partial x} = \frac{v \cdot (\ell) - v}{T} - \ell [v' \cdot (\ell)]^2 \partial \ell / \partial x \tag{5}$$

## 3.0. ZHANG'S SECOND-ORDER TRAFFIC FLOW MODEL AND ITS NUMERICAL SOLUTIONS

A non-equilibrium traffic flow theory was developed by Zhang (1998) and in Zhang (2000a) he developed the Godunov FDE for the model. Zhang's model is a second order model written in the conservation form:

$$\left( \begin{matrix} \ell \\ v \end{matrix} \right)_t + \left( \begin{matrix} \ell v \\ \frac{v^2}{2} + \phi \ell \end{matrix} \right)_x = \left( \begin{matrix} 0 \\ \frac{v_* (\ell) - v}{T} \end{matrix} \right) \tag{6}$$

Where  $\phi(\ell)$  is a velocity flux function and defined as

$$\phi'(\ell) = \frac{c^2(\ell)}{\ell} = \ell (v_*^1(\ell))^2 \tag{7}$$

Here  $c(\ell) = -\ell v_*^1(\ell)$  is the traffic sound speed.

In (1)  $v_*(\ell)$  is the equilibrium speed.

$v_*$  equilibrium traffic speed which is decreasing with respect to traffic density i.e.  $v_*'(\ell) < 0$ .

The fundamental diagram

$q_*(\ell) \equiv \ell v_*(\ell)$  is concave

i.e.  $q_*''(\ell) < 0$

in (1),  $\tau$  is the relaxation time and the relaxation term  $\frac{v_*(\ell) - v}{\tau}$  constrains the difference between the real travel

speed and the equilibrium travel speed  $v_*$

when the relaxation term is 0, Zhang's model reduces to the LWR model.

$$\ell_t + (\ell v_*)_x = 0 \tag{8}$$

Zhang's model has three different wave velocities (relative to the road). A first order wave velocity and two second order wave velocities.

The first-order wave velocity is the wave velocity of the corresponding LWR model:

$$\lambda_*(\ell) = v_*(\ell) = v_*(\ell) + \ell v'_*(\ell) \tag{9}$$

That two second order wave velocities are

$$\lambda_{1,2}(\ell, v) = v \pm C(\ell) = V \pm \ell V_*^1(\ell) \tag{10}$$

The relationship between three wave speed along  $(\ell, v_*)$  phase curve is that

$$\lambda_1 = \lambda_* < \lambda_2 \tag{11}$$

The waves with wave speed  $\lambda_1$  are called 1-waves; the waves with wave speed  $\lambda_2$  is called 2-waves.

Since  $\ell, v \geq 0$  and  $v'_* \leq 0$ , the 2-waves speed  $\lambda_2 > 0$  for any  $\ell, v$ .

Since Zhang's model is hyperbolic system of conservation laws with a relaxation term, the system is stable  $\lambda_1 \leq \lambda_* > \lambda_2$ .

Liu, 1979, 1987 Chen *et al*, 1994.

This condition is satisfied by Zhang's model. Thus Zhang's model is always stable. We now solve (6) numerically by studying Godunov type method and properties of Zhang's model.

**3.1. A Godunov-type finite difference method: a review.**

A Godunov-type FDE for Zhang's model are:

$$\frac{\ell_i^{j+1} - \ell_i^j}{k} + \frac{\ell_{i+1/2}^{*j} v_{i+1/2}^{*j} - \ell_{i-1/2}^{*j} v_{i-1/2}^{*j}}{h} = 0 \tag{12}$$

$$\frac{v_i^{j+1} - v_i^j}{k} + \frac{\frac{(v_{i+1/2}^{*j})^2}{2} + \phi(\ell_{i+1/2}^{*j}) - \frac{(v_{i-1/2}^{*j})^2}{2} - \phi(\ell_{i-1/2}^{*j})}{h} = \frac{v_* \ell_i^{j+1} - v_i^{j+1}}{T} \tag{13}$$

$\ell_i^j$  is the average of  $\ell$  in cell  $i$  at time step  $j$

$$\text{i.e } \ell_i^j = \frac{1}{h} \int_{x_{i-1/2}}^{x_{i+1/2}} \ell(x, t_j) dx \tag{14}$$

$v_i^j$  is the average of  $v$  similarly

$\ell_{i+1/2}^{*j}$  is the average of  $\ell$  through the cell boundary  $x_{i+1/2}$  over the time interval  $(t_j, t_{j+1})$ ,

$$\text{i.e } \ell_{i+1/2}^{*j} = \frac{1}{k} \int_{t_j}^{t_{j+1}} \ell(x_{i+1/2}, t) dt \tag{15}$$

Similarly

$v_{i+1/2}^{*j}, \ell_{i-1/2}^{*j}$  and  $v_{i-1/2}^{*j}$  are boundary averages.

By measuring the source term with values at time  $t_{j+1}$ , then Zhang's model evaluation equations are

$$\ell_i^{j+1} = \ell_i^j - \frac{k}{h} (\ell_{i+1/2}^{*j} v_{i+1/2}^{*j} - \ell_{i-1/2}^{*j} v_{i-1/2}^{*j}) \tag{16}$$

$$v_i^{j+1} = \frac{1}{(1 + \frac{k}{T})} \{ v_i^j - \frac{k}{h} [ \frac{(v_{i+1/2}^{*j})^2}{2} + \phi(\ell_{i+1/2}^{*j}) - \frac{(v_{i-1/2}^{*j})^2}{2} - \phi(\ell_{i-1/2}^{*j}) ] + \frac{k}{T} v_*(\ell_i^{j+1}) \} \tag{17}$$

Provided with traffic conditions  $(\ell, v)$  at times  $t_j$ , traffic conditions at time  $t_{j+1}$  can be calculated if we

know the boundary averages  $\ell_{i+1/2}^{*j}, v_{i+1/2}^{*j}, \ell_{i-1/2}^{*j}, v_{i-1/2}^{*j}$ . The computation of  $(\ell_{i+1/2}^{*j}, v_{i+1/2}^{*j})$  at the

cell boundary  $x_{i+1/2}$  during the time interval  $(t_j, t_{j+1})$  depends on a Riemann problem for (1) with the following initial conditions

$$v_{j+1}(x, t_j) = \begin{cases} U_l & \text{if } x - x_{i+1/2} < 0 \\ U_r & \text{if } x - x_{i+1/2} > 0 \end{cases} \tag{18}$$

Where we define the state variable  $u(x, t) = (\ell, v), v_i^j = (\ell_i^j, v_i^j) = u(x_i, t_j)$  and left and right

states  $U_l = (\ell_l, v_l), U_r = (\ell_r, v_r)$ . In a first order Godunov method, the cell average

$\ell_l = \ell_i^j, v_l = v_i^j$  as the left side or upstream traffic conditions and  $\ell_r = \ell_{i+1}^j, v_r = v_{i+1}^j$  as the right side or downstream conditions.

In a second order Godunov method, we use higher order approximation to the left and right states.

Here we have neglected the relaxation term in (1) when solving the Riemann problem.

The Riemann problem has been discussed by Zhang (1999a) and the solution to the boundary averages are provided there. The solutions are self-similar and can be expressed in the forms.

$$\varphi\left(\frac{x-x_1+\gamma_2}{t}, U_r, U_l\right)$$

### 3.2.1 Solution of the boundary averages.

There are 8-types of wave solutions to the Riemann problem, which are combinations of two 1-waves and two 2-waves. The calculation of boundary averages depends on the type of solutions. The formula for calculating the boundary averages are listed as follows.

1. The solution is a 1-shock when the initial conditions satisfy.

$$H1 : v_2 - v_1 = -\sqrt{\frac{2(\ell_l - \ell_r)(\phi(\ell_l) - \phi(\ell_r))}{\ell_l + \ell_r}} \quad \ell_r > \ell_l, v_r < v_l \quad (19)$$

$$\text{The wave speed is } s = \frac{\ell_r v_r - \ell_l v_l}{\ell_r - \ell_l} \quad (20)$$

The boundary averages  $(\ell_{i+\gamma_2}^{*j}, v_{i+\gamma_2}^{*j})$  are given in the following table

	$\frac{\ell_r v_r - \ell_l v_l}{\ell_r - \ell_l}$	$\ell_{i+\gamma_2}^{*j}$	$v_{i+\gamma_2}^{*j}$
H1	$s > 0$	$\ell_l$	$v_l$
	$s < 0$	$\ell_r$	$v_r$
	$s = 0$	$\frac{\ell_l + \ell_r}{2}$	$\frac{v_l + v_r}{2}$

2. The wave solution is a 2-shock when the initial states satisfy

$$H2 : v_r - v_l = -\sqrt{\frac{2(\ell_l - \ell_r)(\phi(\ell_l) - \phi(\ell_r))}{\ell_l + \ell_r}} \quad \ell_r < \ell_l, v_r < v_l \quad (21)$$

$$\text{The wave speed is } s = \frac{\ell_r v_r - \ell_l v_l}{\ell_r - \ell_l} > 0 \quad (22)$$

The boundary averages  $(\ell_{i+\gamma_2}^{*j}, v_{i+\gamma_2}^{*j})$  are given in the following table

	$s = \frac{\ell_r v_r - \ell_l v_l}{\ell_r - \ell_l}$	$\ell_{i+\gamma_2}^{*j}$	$v_{i+\gamma_2}^{*j}$
H2	$s > 0$	$\ell_l$	$v_l$

3. The wave solution is a 1-rarefaction when the initial state satisfy

$$R1 : v_r - v_l = v_*(\ell_r) - v_*(\ell_l) \quad \ell_r < \ell_l, v_r > v_l \quad (23)$$

The characteristics speed of a 1-rarefaction wave is

$$\lambda_1(\ell, v) = v + \ell v'_*(\ell) \quad (24)$$

The boundary averages are the left state when  $\lambda_1(\ell_l, v_l) > 0$  Similarly they are the right state

when  $\lambda_1(\ell_r, v_r) < 0$  Otherwise,  $(\ell_{i+\gamma_2}^{*j}, v_{i+\gamma_2}^{*j})$  are the solutions of the equations

$$\lambda(\ell_{i+\gamma_2}^{*j}, v_{i+\gamma_2}^{*j}) = \ell_{i+\gamma_2}^{*j} v^*(\ell_{i+\gamma_2}^{*j}) + v_{i+\gamma_2}^{*j} = 0 \quad (25)$$

$$v_{i+\gamma_2}^{*j} - v_l = v_*(\ell_{i+\gamma_2}^{*j}) - v_*(\ell_l) \quad (26)$$

We simplify equations 20 and 21 as

$$\lambda_*(\ell_{i+\frac{1}{2}}^{*j}) = v_*(\ell_l) - v_l \equiv \Delta v \tag{27}$$

$$v_{i+\frac{1}{2}}^{*j} = v_*(\ell_{i+\frac{1}{2}}^{*j}) - \Delta v \tag{28}$$

The boundary averages  $(\ell_{i+\frac{1}{2}}^{*j}, v_{i+\frac{1}{2}}^{*j})$  are as given in the following table.

	$\lambda_1$	$\ell_{i+\frac{1}{2}}^{*j}$	$v_{i+\frac{1}{2}}^{*j}$
R1	$\lambda_1(\ell_l, v_l) > 0$	$\ell_l$	$v_l$
	$\lambda_1(\ell_l, v_l) < 0$	$\ell_r$	$v_r$

4. The wave solution is a 2-rarefaction when the initial states satisfy

$$R2; v_r - v_l = v_*(\ell_l - v_*(\ell_r)), \ell_r > \ell_l, v_r > v_l \tag{29}$$

The characteristic speed of a 2-rarefaction wave is

$$\lambda_2(\ell, v) = v - \ell v'_*(\ell) > 0 \tag{30}$$

The solution of  $(\ell_{i+\frac{1}{2}}^{*j}, v_{i+\frac{1}{2}}^{*j})$  are given in the following table:

	$\lambda_2$	$\ell_{i+\frac{1}{2}}^{*j}$	$v_{i+\frac{1}{2}}^{*j}$
R2	$\lambda > 0$	$\ell_l$	$v_l$

5. The wave solution is a 1-rarefaction + 2-rarefaction when there exists an intermediate state  $(\ell_m, v_m)$  satisfying

$$R1; v_m - v_l = v_*(\ell_m) - v_*(\ell_l), \ell_m < \ell_l, v_m > v_l \tag{31}$$

$$R2; v_r - v_m = v_*(\ell_m) - v_*(\ell_r), \ell_r > \ell_m, v_r > v_m \tag{32}$$

That is to say  $\ell_m$  satisfies

$$2v_*(\ell_m) - v_*(\ell_l) - v_*(\ell_r) - (v_r - v_l) = 0 \tag{33}$$

In which  $\ell_m < \ell_l, \ell_m < \ell_r$  we can write  $v_m$  as  $v_m = v_*(\ell_m) + v_l - v_*(\ell_l)$  (34)

The boundary averages  $(\ell_{i+\frac{1}{2}}^{*j}, v_{i+\frac{1}{2}}^{*j})$  are given as in the table below.

	$\lambda_1$	$\ell_{i+\frac{1}{2}}^{*j}$	$v_{i+\frac{1}{2}}^{*j}$
R1-R2	$\lambda_1(\ell_l, v_l) > 0$	$\ell_l$	$v_l$
	$\lambda_1(\ell_m, v_m) < 0$	$\ell_m$	$v_m$

6. The wave solution is a rarefaction +2 shock when there exists an intermediate state  $(\ell_m, v_m)$  satisfying

$$R1 : v_m - v_l = v_*(\ell_m) - v_*(\ell_l), \ell_m < \ell_l, v_m > v_l \tag{35}$$

$$R2 : v_r - v_m = -\sqrt{\frac{2(\ell_m - \ell_r)(\phi(\ell_m) - \phi(\ell_r))}{\ell_m + \ell_r}}, \ell_r < \ell_m, v_r < v_m \tag{36}$$

That is to say  $\ell_m$  satisfies

$$v_r(\ell_m) - v_*(\ell_l) = \sqrt{\frac{2(\ell_m - \ell_r)(\phi(\ell_m) - \phi(\ell_r))}{\ell_m + \ell_r}} - (v_r - v_l) = 0 \tag{37}$$

In which  $\ell_r < \ell_m < \ell_l$  we can write  $v_m$  as

$$v_m = v_*(\ell_m) + v_l - v_*(\ell_l) \tag{38}$$

The boundary averages  $(\ell_{i+\frac{1}{2}}^{*j}, v_{i+\frac{1}{2}}^{*j})$  are given as followings

	$\lambda_1$	$\ell_{i+\frac{1}{2}}^{*j}$	$v_{i+\frac{1}{2}}^{*j}$
	$\lambda_1(\ell_l, v_l) > 0$	$\ell_l$	$v_l$
R1-H2	$\lambda_1(\ell_m, v_m) < 0$	$\ell_m$	$v_m$

7. The wave solution is a 1-shock + 2-shock when there exists an intermediate state  $(\ell_m, v_m)$  satisfying

$$H1 : v_m - v_l = -\sqrt{\frac{2(\ell_l - \ell_m)(\phi(\ell_l) - \phi(\ell_m))}{\ell_l + \ell_m}}, \ell_m > \ell_l, v_m < v_l \tag{39}$$

$$H2 : v_r - v_m = -\sqrt{\frac{2(\ell_m - \ell_r)(\phi(\ell_m) - \phi(\ell_r))}{\ell_m + \ell_r}}, \ell_r < \ell_m, v_r < v_m \tag{40}$$

That is to say,  $\ell_m$  satisfies

$$-\sqrt{\frac{2(\ell_l - \ell_m)(\phi(\ell_l) - \phi(\ell_m))}{\ell_l + \ell_m}} - \sqrt{\frac{2(\ell_m - \ell_r)(\phi(\ell_m) - \phi(\ell_r))}{\ell_m + \ell_r}} - (v_r - v_l) = 0 \tag{41}$$

In which  $\ell_m > \ell_l, \ell_m > \ell_r$ . We can compute  $v_m$  as

$$v_m = -\sqrt{\frac{2(\ell_l - \ell_m)(\phi(\ell_l) - \phi(\ell_m))}{\ell_l + \ell_m}} + v_l \tag{42}$$

The boundary averages  $(\ell_{i+\frac{1}{2}}^{*j}, v_{i+\frac{1}{2}}^{*j})$  are given in the following table:

	$s = \frac{\ell_l v_m - \ell_l v_l}{\ell_r + \ell_l}$	$\ell_{i+\frac{1}{2}}^{*j}$	$v_{i+\frac{1}{2}}^{*j}$
H1-H2	$s > 0$	$\ell_l$	$v_l$
	$s < 0$	$\ell_m$	$v_m$
	$s = 0$	$\frac{\ell_l + \ell_m}{2}$	$\frac{v_l + v_m}{2}$

### 3.3. A second-order Godunov method

This is a second-order finite difference method for Zhang’s model. This method is a two –stage predictor/ corrector method. In this method (1) is decoupled into two nonlinear scalar equations in each interval  $(x_{i-1/2}, x_{i+1/2})$  at time  $t_j$  and the predictor/corrector procedures are applied to those scalar functions. We can write Zhang’s model as :

$$u_t + A(u) u_x = s(u) \tag{48}$$

Where  $u = \begin{pmatrix} \ell(x,t) \\ v(x,t) \end{pmatrix}$  (49)

And

$$A(u) = \begin{pmatrix} v & \ell \\ \ell v_* & v \end{pmatrix} \tag{50}$$

The two eigen values and corresponding eigen vectors are:

$$\lambda_1(u) = v + \ell v_* (\ell) \quad r_1(u) = [1, v'_*(\ell)]^t \tag{51}$$

$$\lambda_2(u) = v - \ell v'_*(\ell) \quad r_2(u) = [1, -v'_*(\ell)]^t$$

We diagonalize  $A(u)$  by

$$T^{-1}(u) A(u) T(u) = \begin{pmatrix} \lambda_1(u) & 0 \\ 0 & \lambda_2(u) \end{pmatrix} \equiv \wedge(u) \tag{52}$$

Where the transformation matrix  $T(U) = \begin{pmatrix} 1 & 1 \\ v'_*(\ell) & -v'_*(\ell) \end{pmatrix}$  (53)

Letting  $w = T^{-1}(u) u$  Zhang’s model (2000b) under the transformation becomes

$$w_t + \wedge(u) w_x = T^{-1}(u) s(u) \tag{54}$$

For the solution  $w(x, t)$  to a scalar equation  $w_t + \lambda(w) w_x = 0$  the first-order Godunov method uses a step function  $w_1(x, t_j)$  to interpolate the solution, i.e.;

$$w_1(x, t_j) = w_i^j \text{ if } x_{i-1/2} \leq x \leq x_{i+1/2} \tag{55}$$

In a first-order Godunov method the Riemann problem has the following jump initial conditions:

$$\begin{aligned} w_{i+1/2}^{j,L} &= w_i^j \\ w_{i-1/2}^{j,R} &= w_i^j \end{aligned} \tag{56}$$

For a second order Godunov method we interpolate the initial condition with a piece-wise linear function

$$w_1(x, t_j) = w_i^j + \frac{x - ih}{h} \Delta^{VL} w_i^j \text{ if } x_{i-1/2} \leq x \leq x_{i+1/2} \tag{57}$$

Then we do a half step prediction

$$w_{i+1/2}^{j+1/2,L} = w_i^j + 1/2(1 - \lambda(w_i^j) \frac{k}{h}) \Delta^{VL} w_i^j \tag{58}$$

$$w_{i-1/2}^{j+1/2,R} = w_i^j - 1/2(1 - \lambda(w_i^j) \frac{k}{h}) \Delta^{VL} w_i^j$$

Where  $\Delta^{VL} w_i = \begin{cases} S_i, \min(2|w_{i+1} - w_i|, 2|w_i - w_{i-1}|, 1/2|w_{i+1} - w_{i-1}|, \xi) > 0. \text{Zhang (2000a)} \\ 0, \text{otherwise} \end{cases}$

$$S_i = \text{Sign}(w_{i+1} - w_{i-1}) = \tag{59}$$

$$\xi = (w_{i+1} - w_i) \cdot (w_i - w_{i-1}) \tag{60}$$

The Van Leer slope limiter ensures that the method remains second order when the solution  $w(x, t)$  is smooth and eliminates Gibb’s phenomenon at discontinuities.

We apply the procedure above to the two scalar equation of the related homogeneous 2X2 system in (50) to obtain  $w_{i+1/2}^{j+1/2,L}$  and  $w_{i-1/2}^{j+1/2,R}$ . Given the half –step values of  $w_{i+1/2}^{j+1/2,L}$  and  $w_{i-1/2}^{j+1/2,R}$ ,  $U_{i+1/2}^{j+1/2,L}$  and  $U_{i-1/2}^{j+1/2,R}$  can be calculated by an inverse transformation

$$u_{i+1/2}^{j+1/2,L} = T(u_i^j) w_{i+1/2}^{j+1/2,L} \tag{61}$$

$$u_{i-1/2}^{j+1/2,R} = T(u_i^j) w_{i-1/2}^{j+1/2,R}$$

We then solve Riemann problem to find the boundary average

### 3.4. Numerical solution of Zhang’s model

Following the discussions in the preceding sections we carry out some numerical computations to test the validity of the Godunov method and the property of Zhang’s model

We shall use Newell’s equilibrium model

$$v_*(\ell) = v_f (1 - \exp\{-\frac{c_j l}{v_f} (1 - \frac{\ell_1}{\ell})\}) \tag{62}$$

And set  $v_f = 1, c_j = 1, \ell_j = 1$  to get the Standardized equilibrium relationship:

$$v_*(\ell) = 1 - \exp(1 - \frac{1}{\ell}) \tag{63}$$

The domain for  $\ell$  is  $0 \leq \ell \leq 1$ , the range for  $v$  is the same i.e.  $0 \leq v_* \leq 1$ . The traffic flow rate is

$q_* = \ell v_*$ . The equilibrium travel speed  $v_*(\ell)$  and flow rate  $q_*(\ell)$  shown in figure. 1

The sub characteristic, that is the first-order characteristic velocity - the wave velocity of the correspondence L W R model is

$$\lambda_* = 1 - (1 + \frac{1}{\ell}) \exp(1 - \frac{1}{\ell})$$

And the second order eigen values are

$$\lambda_{1,2} = v \pm \frac{1}{\ell} \exp(1 - \frac{1}{\ell})$$

When  $0 \leq \ell \leq 1$ , we have

$$|\lambda_2| < |v| + 1$$

The CFL condition number is defined as:

$$\text{Max} |\frac{k}{h} \lambda_2(\ell, v)| \leq \frac{k}{h} (\text{max } v + 1) \tag{64}$$

Since the CFL number is not larger than 1, we find

$$k \leq \frac{h}{\text{max } v + 1} \tag{65}$$

In all the computations which follow we let  $x \in [0l, 800l]$ , where  $l$  is the unit of length. The number of grid points is denoted by  $N$  and  $h = \frac{800l}{N}$  is the space step. We let  $T_0 = k \tau$  denote the final time ( $\tau$  is the unit of

time) and  $M$  the number of time steps and  $K = \frac{k\tau}{M}$ . From the CFL condition, we have

$$(\frac{\text{max } v + 1}{800}) \frac{kN}{m} \frac{\tau}{l} \leq 1 \tag{66}$$

Setting  $\tau = l = 10.0$ , and  $M=N$ , CFL condition is not violated when  $k \leq 400 \tau$  since  $\text{max } v < 1$ .

#### 3.4.1 Riemann Solution

In the following four computation we use the first order Godunov method to examine different types of waves solution. With four well chosen jump initial condition we observe four different type of waves

$H1 - H2, R1 - R2, R1 - H2$  and  $H1 - R2$ . To prevent the 2-waves from relaxing to 1-waves in a short time, here we rescale the relaxation time  $\tau \rightarrow 1000 \tau$ .

For each computation we prevent a contour plot of both  $\ell$  and  $v$  until  $T_0 = 400 \tau$  and several 2-D waves at different time  $t$  have been selected from the counter plot.

Computation 1. we use the following initial conditions

$$\ell(x, 0) = 0.65 \quad \forall x \in [0L, 800L] \tag{67}$$

$$V(x, 0) = \begin{cases} v_*(0.65) & \forall x \in (0l, 200l) \\ v_* 0/65 - 0.2 & \text{otherwise} \end{cases} \tag{68}$$

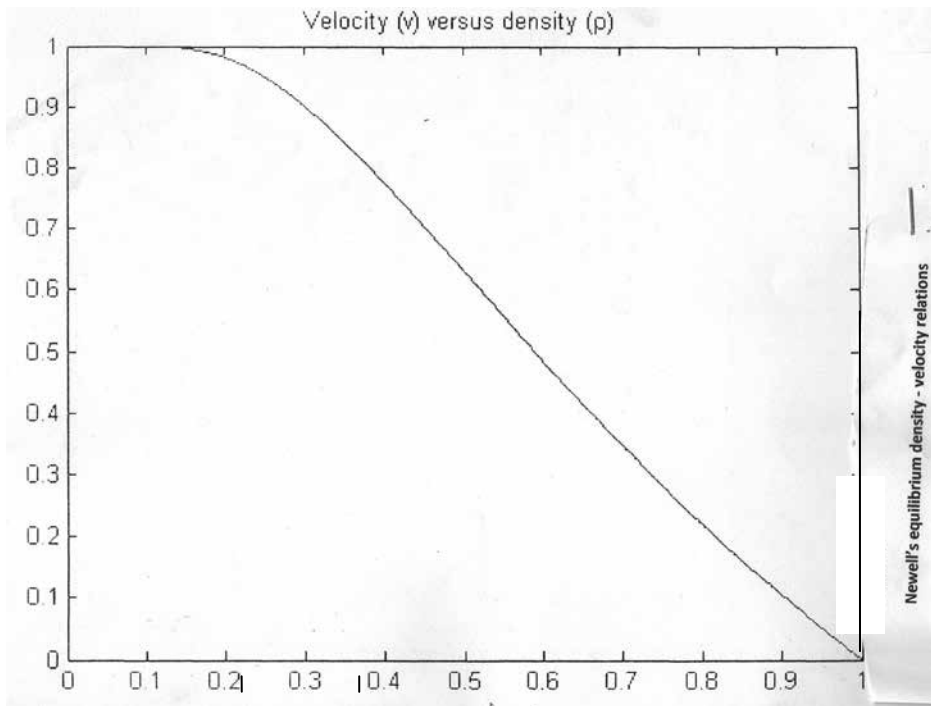


FIGURE 2

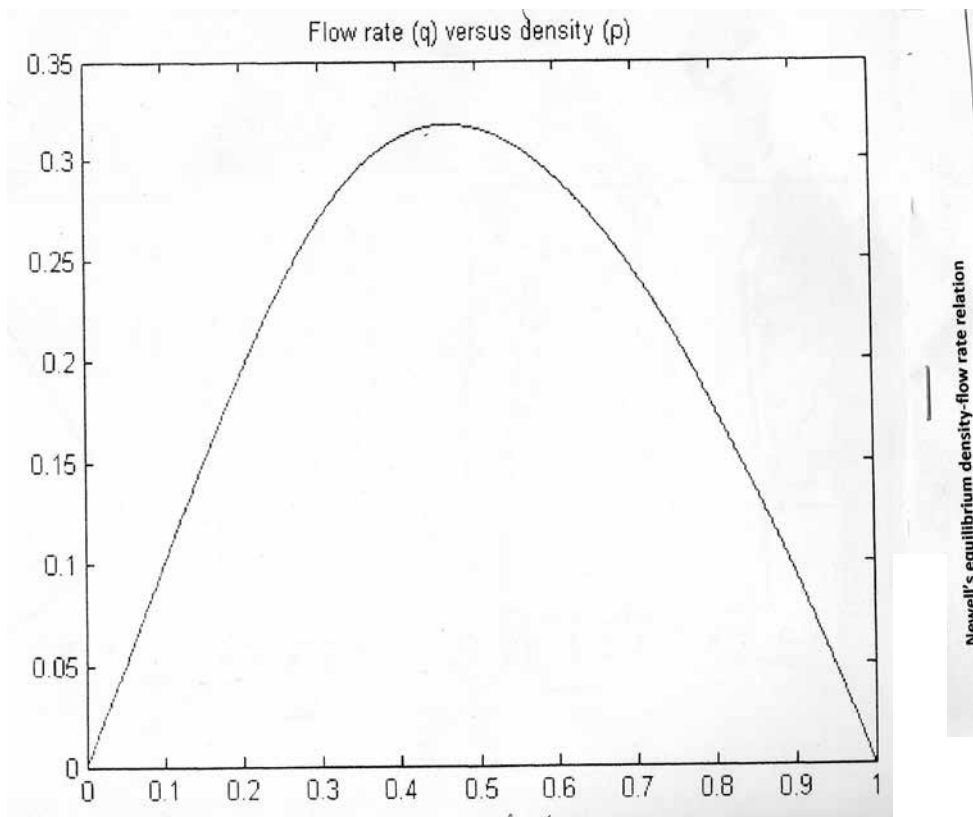


FIGURE 3

3.4.2.A GENERAL SOLUTION AND CONVERGENCE RATES

Using the general initial conditions

$$\ell(x, 0) = 0.65 + (\sin(2\pi x)/8001)/4 \tag{69}$$

$$V(x, 0) = v_* \ell(x, 0) + 0.1 \quad \forall x \text{ in } (0l, 800l) \tag{70}$$

We use the first order Godunov method to obtain the solutions

We now compute the convergence rates for the first and second order methods with Neumann boundary conditions with initial conditions (69),(70)

The convergence rate is calculated from the comparison between the solution on different grids.

The grid numbers  $2N$  and  $N$  generate different grid sizes;  $h/2$  and  $h$ .

The solution at time  $T_0$  is denoted as  $(U_i^{2N})_{i=1}^{2N}$  and  $(U_i^N)_{i=1}^N$  respectively and define the difference vector  $e^{2N-N}$  between these two solutions as  $e_i^{2N-N} = \frac{1}{2} (U_{2i-1}^{2N} + U_{2i}^{2N}) - U_i^N, i = 1, \dots, N$  (71)

Then the relative error between the two solutions is defined as the norm of the difference vector;

$$e^{2N-N} = \|e^{2N-N}\| \tag{72}$$

The convergence rate is defined as

$$r = \log_2(e^{2N-N} / e^{4N-2N}) \tag{73}$$

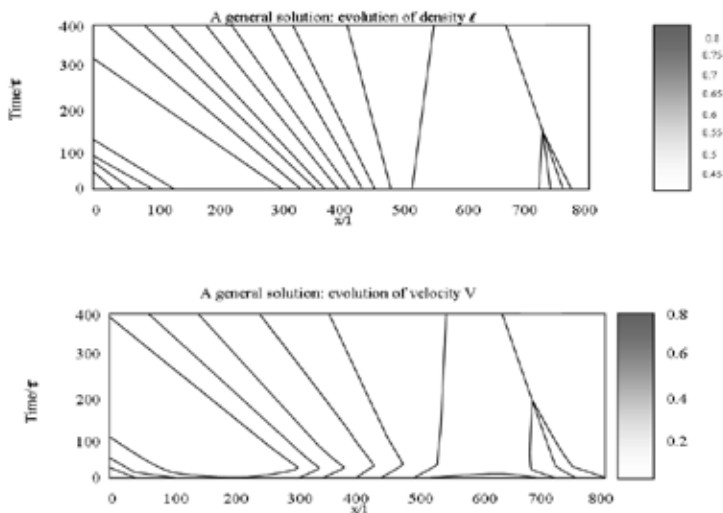


Figure 11.: A General Solution of Zhang's Model with new Neumann BC

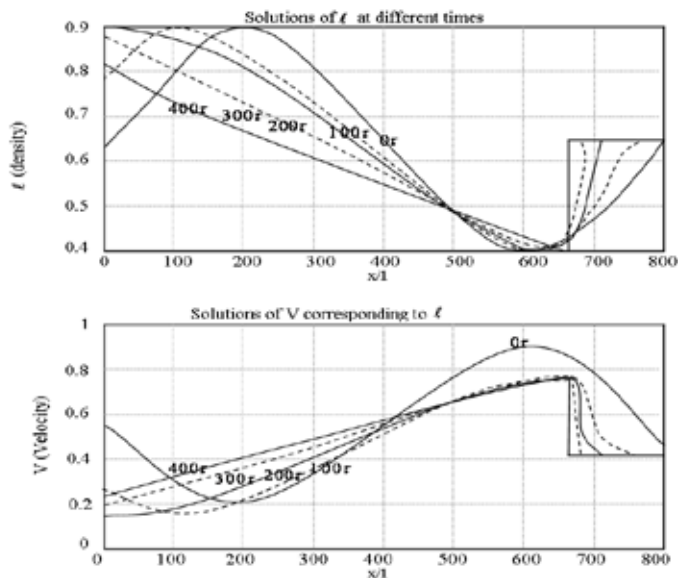


Figure 12.: The Solutions from Figure 11 at selected Times

In (74), the norm can be  $L^1$ -,  $L^2$ -,  $L^3$ - or  $L^\infty$ - norm

For N equal to 32,64,128,256,512,1024 and 2048, the relative errors and convergence rates for the first Godunov method are given in Table (1), and those for second order Godunov's method the convergence rates related to  $L^1$  norm errors and even larger than that related to  $L^\infty$ - norm errors.

From table 1 we also see that the rates for  $\ell$  and  $\nu$  are consistent since  $\ell$  and  $\nu$  are in equilibrium at  $400\tau$ . From Table 2, the convergence rates for the second-order method, although better slightly than those first order method are not second order due to the effect of the relaxation term.

**Rate of Convergence**

Grid Size	L1 Error	Order of Convergence, P
32	1.372733e-09	-
64	4.590219e-10	1.58042
128	1.271022e-10	1.85257
256	3.305757e-11	1.94294
512	8.381246e-12	1.97974

The order of convergence, P is determined as follows

$$P = \frac{\log(E_h / E_{h/2})}{\log 2}$$

where  $E_h$  is the L1 error for the current grid size N and  $E_{h/2}$  is that of the refined mesh

N/2. Therefore, the order of convergence is approximately, P= 2 from the trend in the table.

**REFERENCE**

Algers, S., E. Bernauer, M. Boero, L. Brehert, C. Di Taranto, M. Dougherty, K. Fox and J.F. | Cremer, M., and M.papageorgiou (1981), Parameter Identification for a Traffic Flow Model. Automatic 17,837-843 | Corinne Braban-Ledoux (2000).METACOR-A Macroscopic Modelling Tool for Corridor Application to the Stockholm test site, KFB Contrast (1998-0547), Center for Traffic Engineering and Traffic Simulation. | Esser, J., L. Neubert, J. Wahle, and M. Schivckenberg (1999). Microscopic online Simulation of Urban Traffic Theory, Jerusalem, 517-534. | Hattari, Y, yashimoto, T.,Inoue, S.2012 A study for the traffic flow control considering the capacity of the road by cellular automaton method. | Helbing. (1996). Gas-kinetic derivation of Navier –Stock-like traffic equations. Physical Review E 53(3), 2266-2381. | Hoogendon, S.P.(1999).Multiclass Continuum Modeling of Multiclass Traffic Flow.Ph.D.Thesis T99/5.TRAIL Thesis Series,Delft University Press. | Hoogendoorn, S.P. and P.H.L. Bovy (2000a). Modelling Multiple User-Class Traffic Flow. Transportation Research B (34) 2, 123-146. | Joonsoo Lee; Bvik,A.S. (2009) Estimation and analysis of urban traffic flow | Kerner,B.S.,konhauser,P. ans Schilke,M. (1996) A new approach to problems of Traffic flow theory. In : lesort,J.B.(ed),Proceedings of the 13th international Symposium of Transportation and Traffic Theory,Lyon,119-145. | Kerner,B.S.,(1999).Theory of congested Traffic Flow:Self-organization without Bottlenecks. Proceedings of the 14th International Symposium on Transportation and Traffic Theory,Jerusalem.147-172. | Kerner, B.S, Aleksic, and Rehborn, H. (2000). Automatic Tracing and Forecasting of Moving Traffic Jams using Predictable Features of Congested Traffic Flow. In: Schneider, And U. Becker (eds), Control in Transportation System 2000, Proceedings of the 9th IFAC Symposium, Braunschwig, Germany, 501-506 | Kerner Boris S (2009) on an introduction to Modern traffic flow theory | Kit you chan, Dills, T.S. chang, E 2013 on road sensor systems installed on freeways used to capture traffic flow data for short-term traffic flow predictors, for traffic flow management, to reduce traffic congestion and improve on vehicular mobility. | Lighthill,M.H., and G.B.Whiteam (1995).On Kinematics waves II: a theory of traffic flow on long,crowded roads.Proceedings of the Royal Society of London Series A,229,317-345. | Li Hui;Zu Yanling 2012. The traffic flow study based on Fuzzy-influence diagram theory. Here many factors affecting traffic flow are selected. | Minderhoud,M.M.(1999).Supported Driving:Impacts on motorway Traffic Flow.Dissertation Thesis,Delft University of Technology.Delft University Press. | Nagel,K.,P.Simon,M.Rickert,and J.esser,(1999).Iterated Transportation Simulation for Dallas and Portland.In: Brilon,Huber ,Scheckenberg,and Wallentonwiz (eds),Traffic and Mobility: Simulation,economics,Environment.Springer-Verlag | Payne.H.J.(1971).Models for Freeway Traffic Control,In : Bekey,G.A. (ed),mathematica; Models of Public Systems 1,21-61. | Prigogine,I., and R.herman (1971).Kinetic Theory of vehicular Traffic.american Elsevier New York. | Wu, N., and W. Brilion (1999). Cellular Automata for Highway Traffic flow Simulation. In : Ceder, A. (ed), Proceeding d of in the 14th International Symposium on Transportation and traffic Theory (abbreviated presentations), 1-18. | Zhang, H.M. (1998). Analyses of non- Equilibrium Traffic flow Transportation Research B, Vol. 32(7), 485-498 | Zhang, H. M. (2000). A finite Difference Model of Non-Equilibrium Traffic Flow, to append in Transportation Research B |